NRL Memorandum Report 5280

(2)

Channel Cooling by Turbulent Convective Mixing

J. R. GREIG, R. E. PECHACEK, AND M. RALEIGH

Experimental Plasma Physics Branch
Plasma Physics Division

March 12, 1984

This research was sponsored by the Office of Naval Research and by the Defense Advanced Research Projects Agency (DoD), ARPA Order No. 4395 Amendment No. 11, monitored by the Naval Surface Weapons Center under Contract N60921-83-WR-W0114.

NAVAL RESEARCH LABORATORY
Washington, D.C.

SECURITY CLASSIFICATION OF THIS PAGE

REPORT DOCUMENTATION PAGE

1a. REPORT SECURITY CLASSIFICATION UNCLASSIFIED	1b. RESTRICTIVE MARKINGS
2a. SECURITY CLASSIFICATION AUTHORITY	3. DISTRIBUTION/AVAILABILITY OF REPORT Approved for public release; distribution unlimited.
2b. DECLASSIFICATION/DOWNGRADING SCHEDULE	
4. PERFORMING ORGANIZATION REPORT NUMBER(S) NRL Memorandum Report 5280	5. MONITORING ORGANIZATION REPORT NUMBER(S)
6a. NAME OF PERFORMING ORGANIZATION Naval Research Laboratory 6b. OFFICE SYMBOL (If applicable)	7a. NAME OF MONITORING ORGANIZATION Naval Surface Weapons Center
6c. ADDRESS (City, State and ZIP Code) Washington, DC 20375	7b. ADDRESS (City, State and ZIP Code) Silver Spring, MD 20919
8a. NAME OF FUNDING/SPONSORING ORGANIZATION ONR and DARPA 8b. OFFICE SYMBOL (If applicable)	9. PROCUREMENT INSTRUMENT IDENTIFICATION NUMBER
8c. ADDRESS (City, State and ZIP Code) Arlington, VA 22217 Arlington, VA 22209	10. SOURCE OF FUNDING NOS. PROGRAM ELEMENT NO.: 61153N 62707E PROJECT NO.: 0 TASK NO.: RR011-09-41 OR 40 AA WORK UNIT NO.: 47-0871 47-0922
11. TITLE (Include Security Classification) CHANNEL COOLING BY TURBULENT CONVECTIVE MIXING	
12. PERSONAL AUTHOR(S) J.R. Greig, R.E. Pechacek, and M. Raleigh	
13a. TYPE OF REPORT Interim 13b. TIME COVERED FROM 1979 TO 1983	14. DATE OF REPORT (Yr., Mo., Day) March 12, 1984 15. PAGE COUNT 24
16. SUPPLEMENTARY NOTATION This research was sponsored by the Office of Naval Research and by the Defense Advanced Research Projects Agency (DoD), ARPA Order No. 4395 Amendment No. 11, monitored by the Naval Surface Weapons Center under Contract N60921-83-WR-W0114.	
17. COSATI CODES FIELD / GROUP / SUB. GR.	18. SUBJECT TERMS (Continue on reverse if necessary and identify by block number) Channels, Cooling, Atmosphere, Turbulence

19. ABSTRACT (Continue on reverse if necessary and identify by block number)

Results from a series of experiments are described which show that hot, reduced-density channels in the atmosphere usually cool by a process of turbulent convective mixing. Five different types of channels were created (a) by the interaction of a pulsed CO_2^2 laser with aerosols in the atmosphere, (b) by electric discharges in the atmosphere, (c) by laser-guided, electric discharges in the atmosphere, and (d) and (e) by the absorption of CO_2^2 laser radiation in nitrogen doped with sulfur hexafluoride. For channels in which the energy deposition was almost cylindrically symmetric and axially uniform, (e), the rate of cooling, after reaching pressure equilibrium, was within an order of magnitude of thermal conduction. But for channels in which the energy deposition was asymmetric and/or non-uniform, the rate of cooling was typically one thousand times faster than thermal conduction (for channels whose radius at pressure equilibrium was ~ 1 cm). These channels were seen to be turbulent and to cool by mixing cold, surrounding air into the hot channel. Such turbulence has been explained by Picone and Boris ~~(Ref. 5)~~ in terms of a residual vorticity that is caused by the non-cylindrical energy deposition. (Continues)

20. DISTRIBUTION/AVAILABILITY OF ABSTRACT UNCLASSIFIED/UNLIMITED ☒ SAME AS RPT. ☐ DTIC USERS ☐	21. ABSTRACT SECURITY CLASSIFICATION UNCLASSIFIED
22a. NAME OF RESPONSIBLE INDIVIDUAL J. R. Greig	22b. TELEPHONE NUMBER (Include Area Code) (202) 767-2077 22c. OFFICE SYMBOL Code 4763

DD FORM 1473, 83 APR EDITION OF 1 JAN 73 IS OBSOLETE.

SECURITY CLASSIFICATION OF THIS PAGE

approx. =

19. ABSTRACT (Continued)

A simple empirical formula is deduced relating the rate of cooling (growth of channel envelope) to the radius of the channel at pressure equilibrium and to the ambient sound speed, which indicates that the effect of vorticity/turbulence saturates for variations in the energy deposition of greater than about 2 to 1.

CONTENTS

CHANNEL COOLING BY TURBULENT CONVECTIVE MIXING

I. INTRODUCTION

The propagation of intense particle beams, laser beams, or electric discharges through a gaseous atmosphere can result in the deposition of significant energy along the path through the atmosphere, producing a hot, reduced-density channel. The properties of the channel, in turn, affect the propagation of subsequent portions of the beam which would travel along the same path and the propagation of subsequent discharge strikes.[1,2] As the channel developes, these properties are determined not only by the deposition of energy that creates the channel but also by the rate of cooling. For lightning discharges in the atmosphere the rate of cooling of the hot channel also determines the chemical composition of the products.[3,4] In this paper we describe the results of a series of experiments which show that over a wide range of channel conditions the primary mechanism for channel cooling is turbulent convective mixing. Such turbulence has been explained by Picone and Boris[5,6] in terms of a residual vorticity that is caused by non-cylindrical features in the deposition of energy during the formation of the channel. For channels whose radius after reaching pressure equilibrium with the surrounding atmosphere is ~ 1 cm, cooling by turbulent convective mixing is typically one thousand times faster than thermal conduction which means that channels cool on a time scale of milliseconds rather than seconds.

II. EXPERIMENTAL PROCEDURE

We have studied five different types of channels with very different energy deposition (from 0.4 J/cm^3 to 40 J/cm^3), with radii at pressure equilibrium varying from 0.4 cm to 2.3 cm, and with a wide range of asymmetry in the energy deposition: they are listed in Table 1. None of these channels was created by an intense particle beam but channels were created by the deposition of laser energy in gaseous atmospheres and by ohmic heating in electric discharges.

Type A). Channels of type A were produced in the laboratory atmosphere by CO_2 laser-driven, aerosol-initiated, air-breakdown. The output pulse from a UV preionized, gain-switched TEA laser,[7] consisting of an oscillator and three

Manuscript approved December 21, 1983.

TABLE 1. Channel Cooling Studies

	Energy Deposition	Radius**	Initial Perturbation
A. CO_2 Laser/ Aerosols/ Atmosphere	2	2.3	very large
B. Unguided Electric Discharge	40	1.4	small
C. Laser-guided Electric Discharge	20	1.0	large
D. CO_2 Laser- Off-axis Modes N_2 + SF_6	0.4	0.5	very small
E. CO_2 Laser- Axial Modes/ N_2 + SF_6	0.4	0.4	negligible
	J/cm^3	cm	

*Energy Deposition is measured before expansion.
**Radius is radius after expansion to pressure equilibrium [$r(\tau)$].

amplifiers, was focused by a 3 m focal length salt (NaCl) lens. The radius of the laser beam at focus was ~ 1 cm and over an axial length of ~ 30 cm the radius remained < 1.5 cm. Breakdown occurred in this focal region during the 100 ns spike of the laser pulse and spread towards the lens during the tail of the pulse. Within the focal region breakdown occurred on many individual aerosols (Figure 1). Nearly spherical plamsas were created that grew during the tail of the laser pulse and finally coalesced to form a pseudo-cylindrical channel.[8] The total energy in the CO_2 laser pulse was ~ 1 kJ, the energy absorbed in the focal region was ~ 2 J/cm^3 and absorption occurred before the channel had expanded appreciably. The hot channel produced by the deposition of this laser energy expanded to reach pressure equilibrium at ~ 100 μs when the channel radius was ~ 2.3 cm. Thereafter the channel became very turbulent and the channel envelope expanded as cold air was mixed into the channel (Figure 1).

Type B). Type B channels were produced by normal (unguided) electric discharges in the atmosphere.[4] A small Marx generator with an output voltage of $\lesssim$ 300 kV, risetime $\lesssim$ 100 ns, and stored energy of $\lesssim$ 1000 J was the source for these discharges. The discharge channel length was only ~ 20 cm, the energy deposited was ~ 40 J/cm^3 again calculated on the volume before any expansion had occurred, and the initial asymmetry of these channels was relatively small (Figure 2). Because all the capacitance, most of the inductance, and an appreciable fraction of the resistance (~ 50%) was within the Marx generator itself, these discharges were very reproducible electrically; period ~ 3 μs and peak current ~ 15 kA decaying to < 1 kA in ~ 7 μs.

Type C). Channels of Type C were produced by laser-guided, electric discharges in the atmosphere.[9] The path of these discharges was designated by laser-induced, aerosol-initiated air breakdown using the pulse from a Q-switched Nd:glass laser ($\lesssim$ 100 J in ~ 40 ns). To enhance the laser/atmosphere interaction the aerosol content of the laboratory atmosphere was increased to ~ 10^{-7} gm/cm^3 by burning a small charge of black powder.[10] The small Marx generator, used for Type B channels, was also used as the

source for these discharges. Discharges of length up to 2 m could be produced by these techniques with a laser energy deposition of only ~ 15 J/m within an initial channel of radius ~ 0.5 cm. For a discharge length of 1 m, the energy deposited by the discharge channel was ~ 20 J/cm^3 (~ 350 J/m of channel length): the current in the discharge was a damped sinewave with peak amplitude ~ 10 kA and period ~ 3 μs that decayed to ≤ 1 kA in ~ 7 μs. The use of aerosols to initiate the laser/atmosphere interaction caused these channels to have relatively large initial asymmetries (Figure 3), but not as large as those in Type A channels. These channels reached pressure equilibrium with the surrounding atmosphere ~ 30 μs after initiation of the Marx discharge; the channel radius was ~ 1 cm and the channel temperature was ~ 5000 K. Turbulent cooling became obvious for these channels after ~ 200 μs.

Type D and E). Both Type D channels and Type E channels were produced by the absorption of CO_2 laser radiation in nitrogen doped with ~ 1% sulfur hexafluoride.[11] At low laser intensities absorption of 10.6 μm radiation excites the sulfur hexafluoride molecules but there is only slow vibrational-translational coupling to the nitrogen molecules.[12] However at higher laser intensities[13] ($\gtrsim 10^6$ watt/cm^2) multiply excited molecules are produced and much more rapid heating of the nitrogen occurrs ($p\tau \lesssim 20$ μs Torr). In our experiment a 50 J pulse from the CO_2 laser[7] was focused, using the 3 m focal length salt lens, into a long cylindrical chamber, 30 cm in diameter. The first 2.5 m of the chamber were filled with dry nitrogen, and the next 1.0 m, the interaction zone, was filled with the nitrogen/sulfur hexafluoride mixture. The fill pressure was ~ 900 Torr and the separation of doped from undoped nitrogen was maintained by flowing the gases in at both ends of the chamber and out at a double aperture, two plates about 10 cm apart, that divided the chamber except for the 7.5 cm diameter holes at their centers. Before each laser shot the chamber was evacuated. It was filled with dry nitrogen and the flow pattern was established. Then the sulfur hexafluoride was introduced into the appropriate flow line and after the mixture had filled the interaction zone of the chamber (~ 10 minutes) the experiment could procede.

The difference between these two types of channels was in the structure of the CO_2 laser beam. For Type D channels the oscillator of the CO_2 laser used a simple "plane-plane" cavity. Thus the laser beam contained off-axis modes that came to focus at different off-axis positions. The intensity distribution in the focal region (in the interaction zone) therefore consisted of a number of "hotspots", in filaments running roughly parallel to the optic axis of the lens, with regions of lower intensity between the hotspots.

For Type E channels the oscillator of the CO_2 laser was reconfigured to use an off-axis confocal resonator. In such a geometry only axial modes are produced. Further, the "crescent" shaped output beam produced by the oscillator was masked with a 7.5 cm diameter aperture to select a nearly uniform, circular laser beam. In the focal region of the lens, the energy distribution from this beam was nearly azimuthally symmetric.

Channels produced by these two laser beams are shown in Figure 4. At early times ($\sim$ 100 μs) when the channels have reached pressure equilibrium but turbulence has not had time to grow, the "hot spots" in the laser beam cause the fringes in the interferogram of the Type D channels to contain sharp discontinuities. Fringes in the interferogram of the Type E channels are smooth and continuous. Type E channels did not exhibit turbulence! Apart from the mode structure in the laser beam Type D and Type E channels were very similar. The energy deposited was $\sim$ 0.4 J/cm^3 for both channels for Type D channels the radius of the CO_2 laser beam was $\sim$ 2.5 mm and for Type E channels it was $\sim$ 2.0 mm. At pressure equilibrium the radii of the channels were 5 mm and 4 mm respectively.

III. RESULTS AND DISCUSSION

For each of the five channels used in these experiments the energy was always deposited within a time, t_1, which was short compared to hydrodynamic times and within a radius r(1) which was $\sim$ 1.0 cm. Thus at time t_1 there existed a hot channel whose density was still the ambient density but whose pressure was significantly above ambient. In the next few tens of microseconds, $\tau \sim 30$ μs, the channel expanded almost adiabatically to reach pressure equilibrium with the surrounding atmosphere. A shock wave was created during this expansion and, in some cases, some energy was lost to

radiation, but these were relatively small corrections ($\lesssim$ 20 %). If the channel had been cylindrically symmetric, as it expanded to pressure equilibrium, it would have cooled thereafter only by thermal conduction. Then the envelope of the channel would have grown as[14]

$$r^2(t) \sim r^2(\tau) + 4\ \alpha_0\ (t - \tau) \quad ,$$

where α_0 is the thermal diffusivity which is $\sim$ 0.2 cm^2/s and $t = \tau$ is the time at which the channel achieved pressure equilibrium. For a channel whose temperature, $T(\tau)$ is $\sim$ 3000 K, the time required for the channel to cool to $\sim$ 600 K, i.e., for the channel radius to increase by a factor of $\sim \sqrt{2}$, is almost one second.

The measured growths of the five channels used in the study are shown in Figure 5. At early times the curve for each channel is linear so that unique values of a maximum anomalous diffusivity, α, can be determined. This initial rate of growth increases with the initial radius of the channel, $r(\tau)$. At later times, channels A through D grow at increasingly slower rates (for B this flattening of the curve occurs between 20 and 30 ms).

Channels of Type E show very little growth compared to other channels, though it is still $\sim$ 10 times thermal conduction. For these channels the slope increased at later times to $\sim$ 5 cm^2/s.

Turbulence transports fluid properties by small scale convection. However in very simple terms, this effect may be modeled as an anomalous diffusion[15] in which fluid cells move a distance ℓ (Prandtl eddy length) before breaking up and losing their identity. The product of this "mean free path" and the relative velocity of the fluid cell is the eddy diffusivity and becomes the effective mass diffusivity, kinematic viscosity, or thermal diffusivity. Thus we expect the thermal diffusivity to be of the form

$$\alpha \sim \ell v$$

where ℓ is a characteristic length and v is a characteristic velocity. For our channels, which are to a first approximation cylindrical, the diffusion is radial. The maximum value of ℓ is therefore some fraction of the radius of the channel, $r(\tau)$. The maximum cell velocity is limited to some fraction of

the sound speed, c_s, of the ambient atmosphere around the channel for that is the maximum speed with which the cold fluid cells can move. With this in mind we have fitted the data for channels A through D to the relation

$$\alpha = c_s \, r(\tau)/k,$$

and find that

$$k = 66 \pm 6.$$

It is perhaps coincidental that the initial growth (cooling) of these four very different channels should be related in such a simple way. Certainly Picone and Boris[5,6] have shown that the residual vorticity, K, developed in different models for the asymmetric energy deposition is always of the form

$$K \sim u_m^2 \, 2 \, \frac{r(\tau) - r(1)}{c_s} \cdot \ln (\rho_\infty/\rho_0) \cdot f$$

where u_m is a characteristic velocity of the expanding channel boundary, ρ_∞ is the ambient density, ρ_0 is the minimum density in the channel, and f is a geometric form factor which is ≤ 1. And this vorticity leads to a predicted maximum anomalous diffusivity of

$$\alpha \sim c_s \, \{r(\tau) - r(1)\} \ln (\rho_\infty/\rho_0) \cdot |f|/4\pi \quad .$$

While values of the maximum anomalous diffusivity calculated from this equation[4,5,6] fall within a small factor ($\lesssim 3$) of the measured values they do not indicate the near constant value of k. Also whereas in the experiments we see a fully developed isotropic turbulence, both theory and the numerical simulations actually deal with a residual, large scale vorticity and do not attempt to reproduce the cascade to fine scale turbulence. On the other hand the near constant value of k in the experiments suggests that the turbulence developed in the channels saturates at relatively modest levels of asymmetry in the energy deposition. However the drastic reduction in the turbulence seen in the Type E channels, and predicted from the theory in that $f \to 0$ for these channels, is a clear indication that development of residual vorticity because of asymmetry in the energy deposition, is the mechanism that causes turbulent convective mixing.

IV. CONCLUSION

In a series of experiments we have found that hot, reduced-density channels in the atmosphere or in nitrogen at near normal temperature and pressure always cool by turbulent convective mixing provided there is more than some minimal level of asymmetry in the channel. The channels were produced by aerosol initiated, CO_2 laser driven air breakdown, by normal electric discharges in the atmosphere, by laser-guided, electric discharges in the atmosphere, and by the absorption of CO_2 laser radiation in nitrogen doped with sulfur hexafluoride. Unfortunately quantitative measurement of the azimuthal asymmetry in the channel was not possible, but it was clearly shown that elimination of the asymmetry prevented the development of turbulent convective mixing. Thus as noted by Picone and Boris[4,5,6] their theory for the development of vorticity and turbulent convective mixing and these experimental findings are in good agreement both in terms of identification of the mechanism for generating turbulence and in the calculation of the magnitude of the effect.

However in the experiments we have found that the anomalous diffusivity, by which the effects of turbulent convective mixing can be represented, saturates at very modest levels of asymmetry in the channel at a value dependent only on the sound speed in the ambient atmosphere and the size of the channel at pressure equilibrium. This phenomenon may well be associated with the fact that the fastest convection is always associated with the largest cells but it is not as yet predictable from the theory. It is certainly convenient that the effect of turbulent convective mixing can be represented so simply for it permits ready inclusion of this effect in channel cooling problems. For channels in the atmosphere with radius at pressure equilibrium of ~ 1 cm, the saturated anomalous diffusivity caused by turbulent convective mixing is ~ 500 cm^2/s and that is ~ 2000 times larger than the effect of thermal conduction.

V. ACKNOWLEDGMENT

These experiments would not have been possible without the technical assistance provided by Messrs E. Laikin and the late James W. Cheadle. The interpretation and understanding of the results has benefitted considerably from many discussions with our colleagues at NRL particularly Drs. J.M. Picone, J.P. Boris, R.F. Fernsler, G. Joyce, and M. Lampe.

This work was supported by the Office of Naval Research and by the Defense Advanced Research Projects Agency.

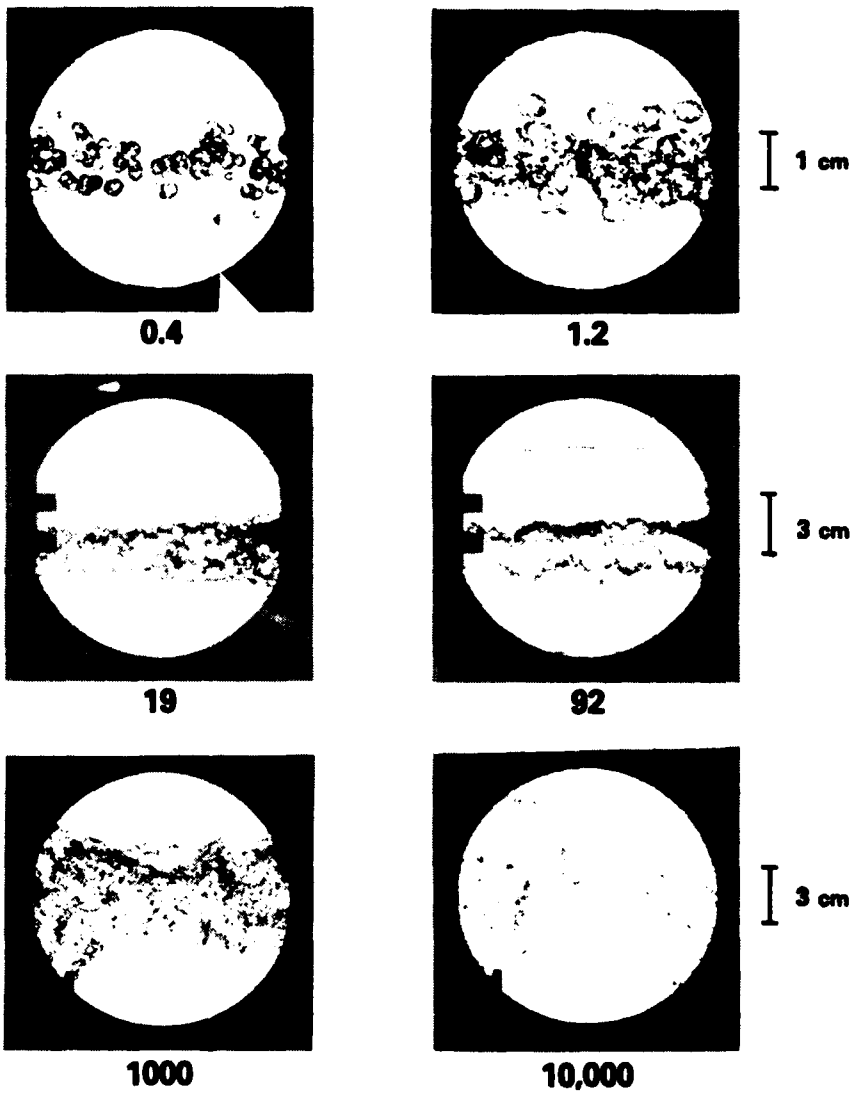

Figure 1. Schlieren photographs of hot channels in the atmosphere produced by aerosol-initiated, laser-driven air breakdown using a pulsed CO_2 laser. Each photograph is from a different laser pulse and the time in microseconds between firing the CO_2 laser and taking the photograph is shown under each photograph. The scale size for each pair of photographs is also indicated. The exposure time for each photograph is ~ 25 ns. The CO_2 laser enters from the left.

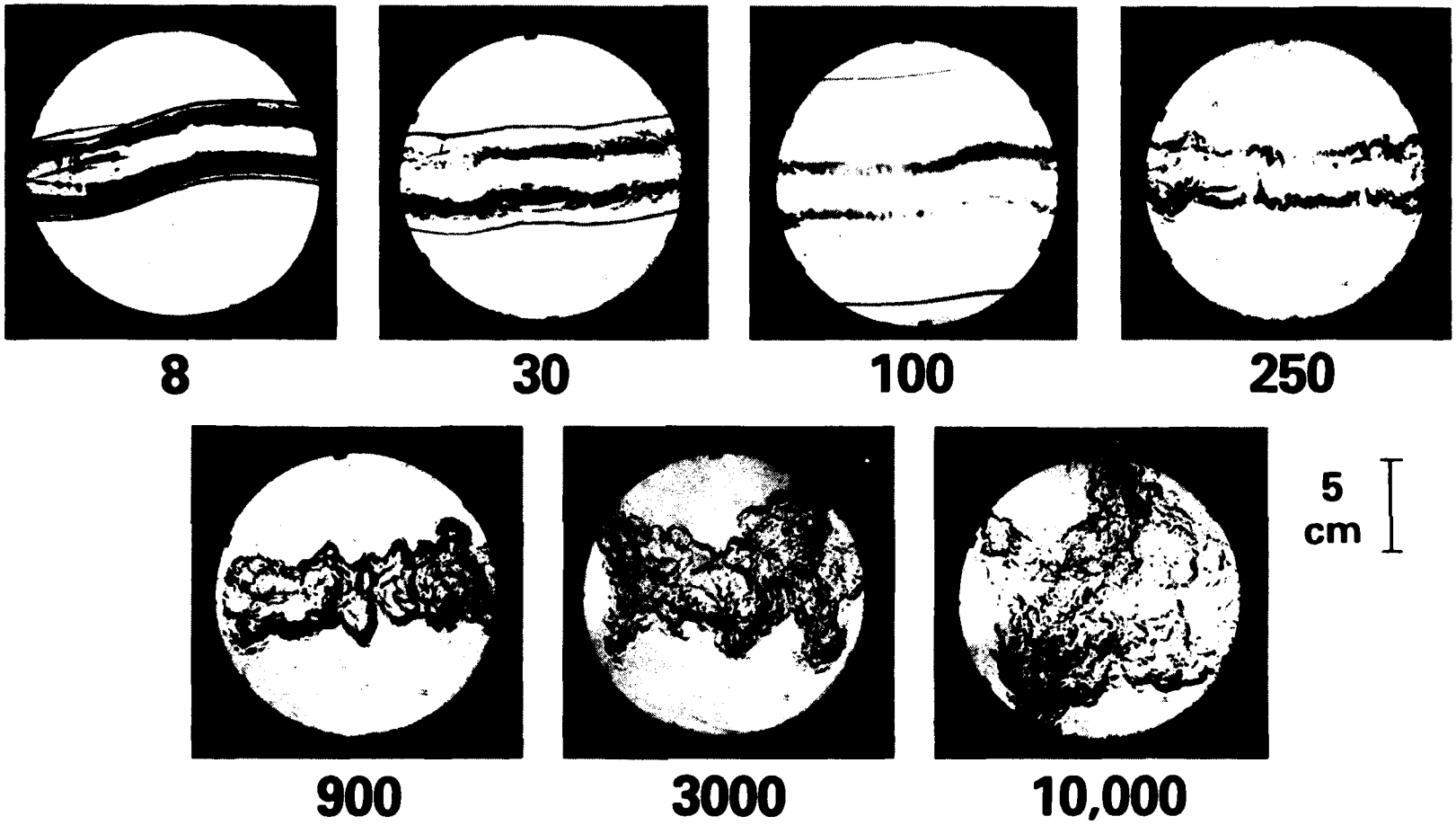

Figure 2. Schlieren photographs of channels produced by normal (unguided) electric discharges in the atmosphere. Each photograph is from a different discharge and the time in microseconds between firing the discharge and taking the photograph is shown under each photograph. The scale size for all photographs is shown on the right. The exposure time is ~ 25 ns. (This sequence was published previously in Reference 4.)

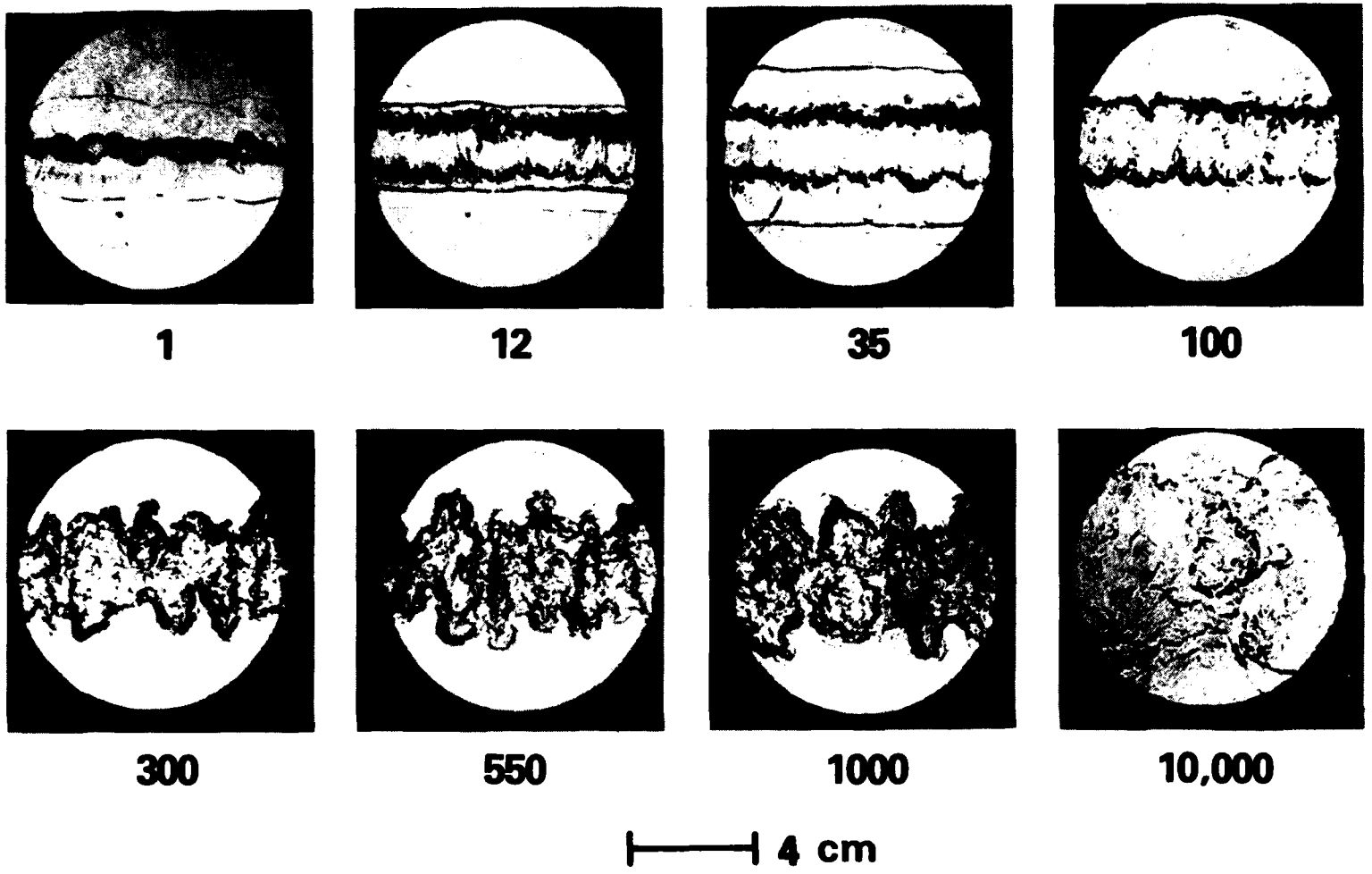

Figure 3. Schlieren photographs of channels produced by laser-guided electric discharges in the atmosphere. Each photograph is from a different discharge and shows the center section of a 1 m long discharge channel. The time in microseconds between firing the discharge and taking the photograph is shown under each photograph. The scale size for all photographs is shown and the exposure time was ~ 25 ns.

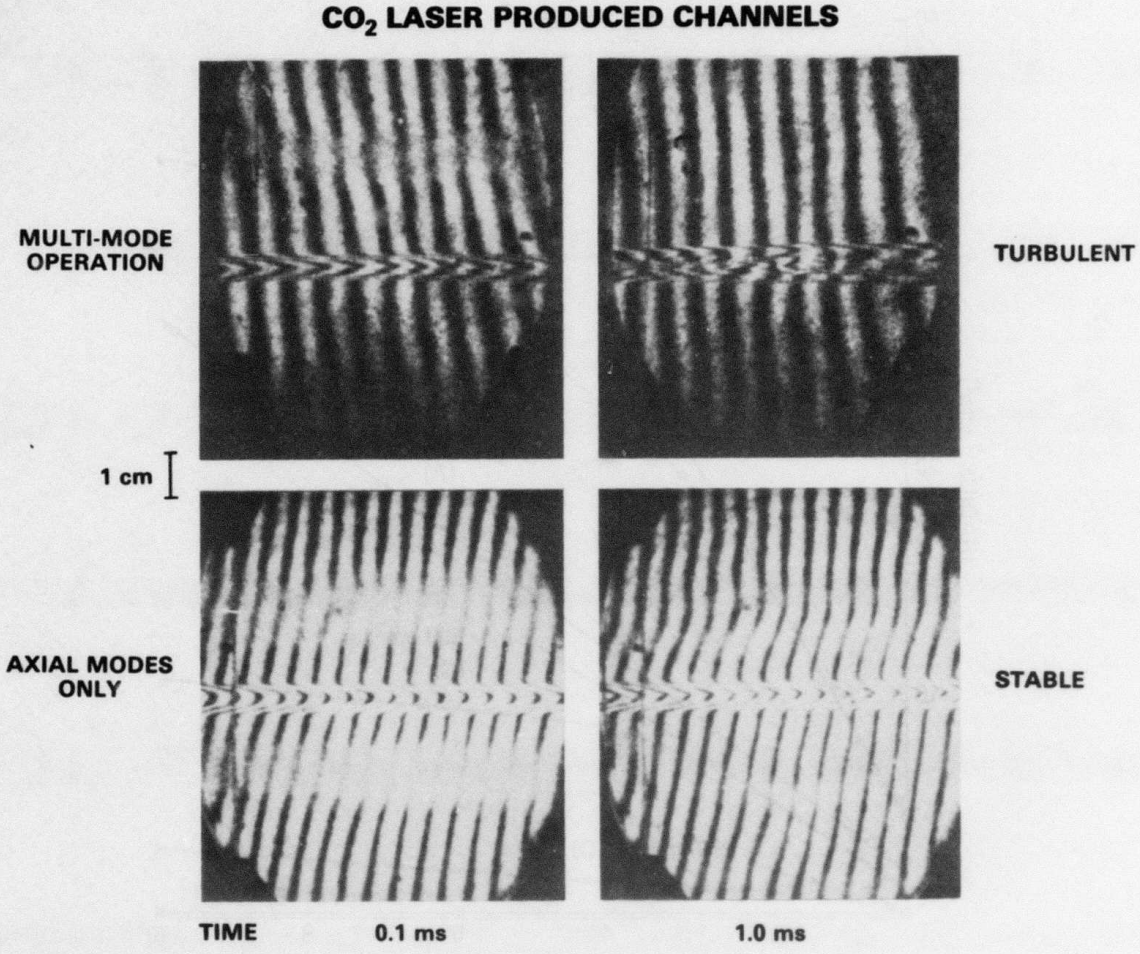

Figure 4. Interferograms of channels produced by the absorption of radiation from a pulsed CO_2 laser in nitrogen doped with ~ 1 % sulfur hexafluoride. The two upper photographs show the first and the tenth frames from a "movie" of a Type D channel. The two lower photographs show the same frames from a "movie" of the Type E channel. These movies were taken with a high speed framing camera using a Mach-Zehnder interferometer and a He:Ne laser. The exposure time is ~ 40 μs and the time between frames was ~ 60 μs (i.e., 10^4 frames/sec). The size scale for these photographs is indicated.

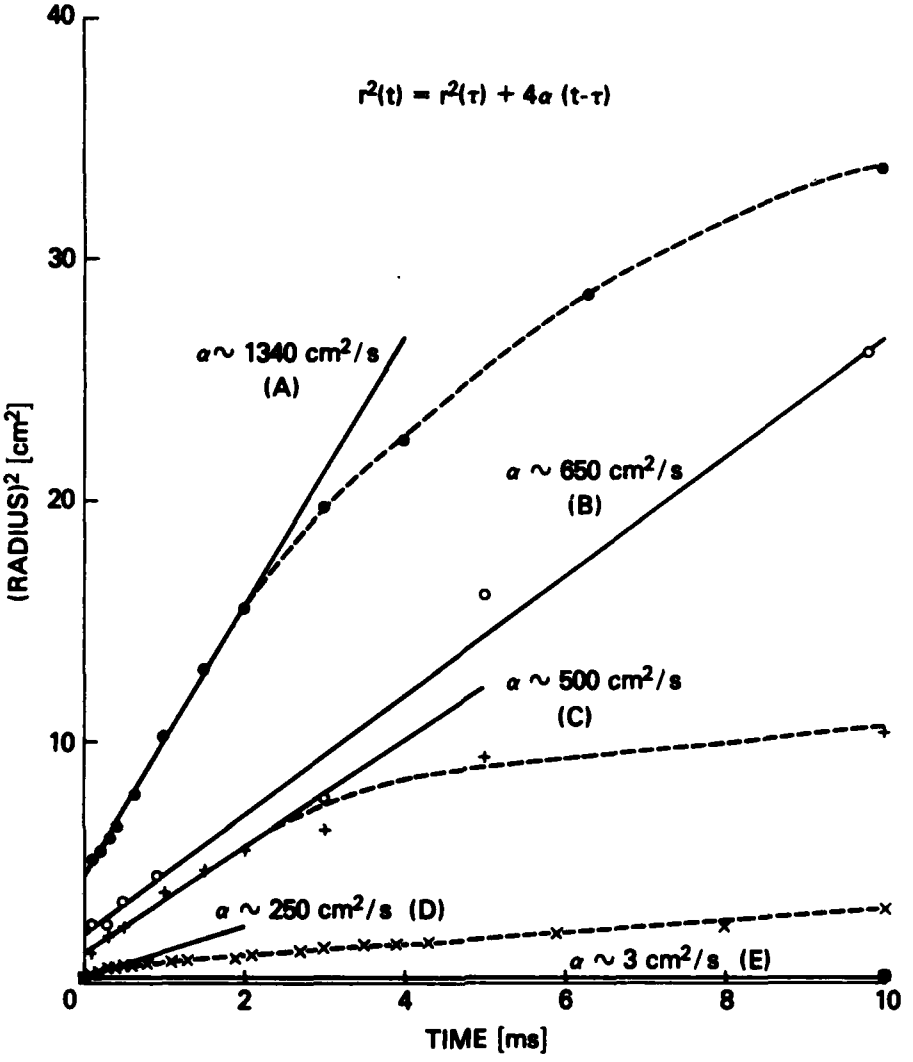

Figure 5. Variation of the measured radius of various channels with time. The channel designations A, B, C, D, and E follow from Table 1. Values of α consistent with the equation

$$r^2(t) = r^2(\tau) + 4\alpha(t-\tau)$$

where $\tau \lesssim 100$ μs are given for the linear portion of each curve.

●	Channel A	Experimental data points.
○	Channel B	
+	Channel C	
×	Channel D	
■	Channel E	

REFERENCES

1. K. Berger, in "Lightning" Edited by R.H. Golde, Academic Press, New York, 1977 Volume 1, p. 182.

2. L.E. Salanave, "Lightning and its Spectrum" University of Arizona Press, Tucson, 1980 p. 50 and 60.

3. R.D. Hill, R.G. Rinker, and H.D. Wilson, J. Atmos. Sci., 37, 179-92 (1980).

4. J.M. Picone, J.P. Boris, J.R. Greig, M. Raleigh, and R.F. Fernsler, J. Atmos. Sci. 38, 2056-62 (1981).

5. J.M. Picone and J. P. Boris, Phys. Fluids 26, 365-82 (1983).

6. J.M. Picone, J.P. Boris, J.H. Gardner, J.R. Greig, M. Raleigh, M. Lampe, R.E. Pechacek, and R.F. Fernsler, Proc. 5th Int. Conf. on High Power Particle Beams, San Francisco, September 1983. (Unpublished)

7. R.E. Pechacek, J.R. Greig, M. Raleigh and S.R. Rod, NRL Memorandum Report 3602, September 1977.

8. J.R. Greig, R.E. Pechacek, R.F. Fernsler, I.M. Vitkovitsky, A.W. DeSilva and D.W. Koopman, NRL Memorandum Report 3647, November 1977.

9. J.R. Greig, R.F. Fernsler, D.P. Murphy, R.E. Pechacek, J.M. Perin, and M. Raleigh, Proc. 7th Int. Conf. on Gas Discharges and Their Applications, London, Sept. 1982, p. 464. [See also, M. Raleigh, J.R. Greig, R.E. Pechacek, and E. Laikin, NRL Memorandum Report 4380, February 1981.]

10. FFFg Superfine Black Rifle Powder, manufactured by GOEX Inc., Moosic, PA 18507.

11. J.R. Greig, R.E. Pechacek, M. Raleigh, and K.A. Gerber, NRL Memorandum Report 4826 (1982). ADA116 408

12. A.V. Nowak, and J.L. Lyman, J. Quant Spectrosc. Radiat. Transfer 15, 945-61 (1975).

13. S.A. Akhmanov, V.M. Gordienko, A.V. Mikheenko and V. Ya. Panchenko, JETP Lett. 26, 453-6 (1977).

14. "Handbook of Physics," Edtd. by E.U. Condon and H. Odishaw, McGraw Hill, New York, 1967 p. 5-64. [See also M. Raleigh, NRL Memorandum Report 4555 (1981) - unpublished.]

15. J.O. Hinze, "Turbulence," McGraw Hill, New York, 1975 p. 361.

DISTRIBUTION LIST

1. Dept. of the Navy
   Chief of Naval Operations
   Washington, D.C. 20350
   ATTN: Dr. C. F. Sharn (op 987)

2. Commander
   Naval Sea Systems Command
   Department of the Navy
   Washington, DC 20363
   ATTN: NAVSEA/PMS 405 (Dr. Finkleman)

3. Air Force Weapons Laboratory (NTYP)
   Kirtland Air Force Base
   Albuquerque, New Mexico 87117
   ATTN: Maj. James Head
   Dr. David Straw

4. U.S. Army Ballistics Research Laboratory
   Aberdeen Proving Ground, Maryland 21005
   ATTN: Dr. D. Eccleshall (DRDAR-BLB)

5. Ballistic Missile Defense Advanced Technology Center
   P. O. Box 1500
   Huntsville, Alabama 35807
   ATTN: Dr. L. Harvard (BMDSATC-1)

6. B-K Dynamics Inc.
   15825 Shady Grove Road
   Rockville, Maryland 20850
   ATTN: Dr. R. Linz

7. Lawrence Livermore Laboratory
   University of California
   Livermore, California 94550
   ATTN: Dr. R. J. Briggs
   Dr. T. Fessenden
   Dr. W. Barletta
   Dr. D. Prono

8. Mission Research Corporation
   735 State Street
   Santa Barbara, California 93102
   ATTN: Dr. C. Longmire
   Dr. N. Carron

9. Pulse Sciences Inc.
   Suite 610
   1615 Broadway
   Oakland, California 94612
   ATTN: Dr. S. Putnam

10. Science Applications, Inc.
    Security Office
    5 Palo Alto Square, Suite 200
    Palo Alto, California 94304
    ATTN: Dr. R. R. Johnston
    Dr. Leon Feinstein

11. Naval Surface Weapons Center
    White Oak Laboratory
    Silver Spring, Maryland 20910
    ATTN: Mr. R. J. Biegalski
    Dr. R. Cawley
    Dr. J. W. Forbes
    Dr. C. M. Huddleston
    Dr. H. S. Uhm
    Dr. R. B. Fiorito

12. C. S. Draper Laboratories
    555 Technology Square
    Cambridge, Massachusetts 02139
    ATTN: Mr. E. Olsson

13. Physical Dynamics, Inc.
    P. O. Box 1883
    LaJolla, California 92038
    ATTN: Dr. K. Brueckner

14. Office of Naval Research
    Department of the Navy
    Arlington, Virginia 22217
    ATTN: Dr. W. J. Condell (Code 421)

15. Avco Everett Research Laboratory
    2385 Revere Beach Pkwy.
    Everett, Massachusetts 02149
    ATTN: Dr. R. Patrick
    Dr. Dennis Reilly

16. Defense Technical Information Center
    Cameron Station
    5010 Duke Street
    Alexandria, Virginia 22314 (2 copies)

17. Naval Research Laboratory
Washington, D. C. 20375
ATTN: T. Coffey - Code 1001
M. Lampe - Code 4792
M. Friedman - Code 4700.1
J. R. Greig - Code 4763 (50 copies)
I. M. Vitkovitsky - Code 4701
W. R. Ellis - Code 4000
S. Ossakow, Supt. - 4700 (26 copies)
Library - Code 2628 (20 copies)
A. Ali - Code 4700.1T
D. Book - Code 4040
J. Boris - Code 4040
S. Kainer - Code 4790
A. Robson - Code 4760
M. Picone - Code 4040
M. Raleigh - Code 4763
R. Pechacek - Code 4763
J. D. Sethian - Code 4762
K. A. Gerber - Code 4762
G. Joyce - Code 4790
D. Colombant - Code 4790
B. Hui - Code 4790

18. Defense Advanced Research Projects Agency
1400 Wilson Blvd.
Arlington, Virginia 22209
ATTN: Dr. J. Mangano
Lt. Col. R.L. Gullickson

19. JAYCOR
205 S. Whiting St.
Alexandria, Virginia 22304
ATTN: Dr. R. Hubbard
Dr. R. Fernsler

20. Mission Research Corp.
1720 Randolph Road, S. E.
Albuquerque, New Mexico 87106
ATTN: Dr. Brendan Godfrey

21. Princeton University
Plasma Physics Laboratory
Princeton, New Jersey 08540
ATTN: Dr. F. Perkins, Jr.

22. McDonnell Douglas Research Laboratories
Dept. 223, Bldg. 33, Level 45
Box 516
St. Louis, Missouri 63166
ATTN: Dr. Michael Greenspan
Dr. J. C. Leader

23. Cornell University
Ithaca, New York 14853
ATTN: Prof. David Hammer

24. Sandia Laboratories
Albuquerque, New Mexico 87185
ATTN: Dr. Bruce Miller, 4255
Dr. Carl Ekdahl
Dr. M. Mazarakis

25. Naval Air Systems Command
Washington, D. C. 20361
ATTN: Dr. J. Reif, Code AIR-350F

26. Beers Associates, Inc.
P. O. Box 2549
Reston, Virginia 22090
ATTN: Dr. Douglas Strickland

27. U. S. Department of Energy
Washington, D. C. 20545
Office of Fusion Energy, ATTN: Dr. W. F. Dove
Office of Inertial Fusion, ATTN: Dr. Richard L. Schriever

Director
U.S. Department of Energy
ER20:GTN, High Energy and Nuclear Physics
Attn: Dr. T. Godlove
Washington, DC 20545

28. AFOSR/NP
Bolling Air Force Base, Bldg. 410
Washington, D. C. 20331
ATTN: Capt. H. Pugh

29. Foreign Technology Division
Wright Patterson AFB, OH 45433
ATTN: Mr. C. J. Butler/TQTD

30. Aerospace Corp.
P. O. Box 92957
Los Angeles, CA 90009
ATTN: Dr. A. Christiansen A6/2407
Dr. E. Frazier

31. SRI International
333 Ravenswood Avenue
Menlo Park, CA 94025
ATTN: Dr. D. Eckstrom

32. Los Alamos National Laboratory
Los Alamos, NM. 87545
ATTN: Dr. T. P. Starke, M-2

33. G T Devices
5705 General Washington Drive
Alexandria, VA 22312
ATTN: Dr. D. A. Tidman
Dr. S. A. Goldstein